A zebrafish embryo screen utilizing gastrulation for identification of anti-metastasis drugs

Joji Nakayama[1,2,3,§], Hideki Makinoshima[1,4] , and Zhiyuan Gong[3]

[1]Tsuruoka Metabolomics Laboratory, National Cancer Center, Tsuruoka, Japan

[2]Shonai Regional Industry Promotion Center, Tsuruoka, Japan.

[3]Department of Biological Science, National University of Singapore, Singapore

[4]Division of Translational Research, Exploratory Oncology Research and Clinical Trial Center, National Cancer Center, Kashiwa, Japan.

[§]Corresponding authors:

Joji Nakayama

Tsuruoka Metabolomics Laboratory, National Cancer Center, Mizukami 246-2, Kakuganji, Tsuruoka, Yamagata, Japan 975-0052.

E-mail: zmetastasis@gmail.com

ORCID: 0000-0003-1077-140X

Tel: +81-235-64-0980

Keywords: Metastasis, gastrulation, EMT, Phenotyping screening, zebrafish

Total words excluding references and figure legends: 2158

Number of figures: 4

Number of tables: 1

Abstract

Few models exist that allow for rapid and effective screening of anti-metastasis drugs. Here, we present a phenotype-based chemical screen utilizing gastrulation of zebrafish embryos for identification of anti-metastasis drugs. Based on our hypothesis that small molecules which interrupt zebrafish gastrulation might suppress metastasis progression of cancer cells, we designed a drug screening concept which uses epiboly, the first morphogenetic movement in gastrulation, as a marker. The screen only needs zebrafish embryos and enables 100 chemicals to be tested in five hours through just observing epiboly progression of a test chemical-treated embryos. In the screen, embryos at two-cell stage are firstly corrected and then developed to sphere stage. The embryos are treated with a test chemical and incubated in the presence of the chemical until vehicle-treated embryos develop to 90% epiboly stage. Finally, positive 'hit' chemicals that interrupt epiboly progression are selected through comparing epiboly progression of a test chemical-treated embryos with that of vehicle-treated embryos under a stereoscopic microscope. Previous study subjected 1280 FDA-approved drugs into the screen and identified Adrenosterone and Pizotifen as epiboly-interrupting drugs. Mouse models of metastasis validated that the drugs could suppress metastasis of breast cancer cells. Furthermore, the screen can be diverted to a chemical genetic screening platform for identification of metastasis-promoting genes. Hydroxysteroid (11-Beta) Dehydrogenase 1 (HSD11b1) and serotonin receptor 2C (HTR2C), which are primary target of Adrenosterone and Pizotifen respectively, induces epithelial-mesenchymal transition (EMT) and promote metastasis of breast cancer cells.

Introduction

Cancer research using zebrafish as a model has attracted attention because this model offers many unique advantages that are not readily provided by other animal models. Moreover, the zebrafish system has been increasingly recognized as a platform for chemical screening because it provides the advantage of high-throughput screening in an in vivo vertebrate setting with physiologic relevance to humans [1-4].

Metastasis is responsible for approximately 90% of cancer-associated mortality. It proceeds through multiple steps: invasion, intravasation, survival in the circulatory system, extravasation, colonization, and metastatic tumor formation in secondary organs with angiogenesis [5-7]. Dissemination of cancer cells is an initial step of metastasis and its molecular mechanism involves local breakdown of basement membrane, loss of cell polarity, and induction of EMT [8,9]. These cellular, biological phenomena are also observed during vertebrate gastrulation in that evolutionarily conserved morphogenetic movements of epiboly, internalization, convergence and extension progress [10]. In zebrafish, the first morphogenetic movement, epiboly, is initiated at approximately four hours post fertilization (hpf) to move cells from the animal pole to eventually engulf the entire yolk cell by 10 hpf. These movements are governed by the molecular mechanisms that are induced by temporally and spatially regulated gene expression, and these mechanisms and changes in gene expression are partially observed in metastatic progression.

Development of the protocol

At least fifty common genes were shown to be involved in both gastrulation and metastasis progression (Table 1) [11-15]. The fifty genes are expressed in xenopus or zebrafish embryos, and genetic inhibition of each of the fifty genes in these embryos interferes with gastrulation progression. Conversely, the same fifty genes are ectopically expressed in metastatic cancer cells and confer metastatic properties on cancer cells, and genetic inhibition of each of the same fifty

genes suppresses metastasis progression. This evidence led us to hypothesize that small molecules which interfere with zebrafish gastrulation might suppress metastasis progression of cancer cells. Based on the hypothesis, we designed a drug screening concept which uses epiboly, the first morphogenetic movement in gastrulation, as a marker. This screen measures suppressor effect of each of chemicals based on epiboly progression of zebrafish embryos (Fig. 1 and 2).

Applications of the method

This screen enables 100 chemicals to be tested in five hours and succeeds to identified two FDA-approved drugs and one crude drug have suppressor effects on metastasis. Adrenosterone and Pizotifen, which were the identified drugs, were validated to suppress metastasis of breast cancer cells in mouse models of metastasis (Fig. 3) [16,17]. Cinnamon bark extract, which was the identified crude drug, was validated to suppress metastatic dissemination of breast cancer cells in zebrafish xenograft model [18]. Furthermore, this screen can be diverted to a chemical genetic screening platform for identification of metastasis-promoting genes. Hydroxysteroid (11-Beta) Dehydrogenase 1 (HSD11b1) and serotonin receptor 2C (HTR2C), which are primary target of Adrenosterone and Pizotifen respectively, induces epithelial-mesenchymal transition (EMT) and promote metastasis of breast cancer cells (Fig. 4) [16,17].

Comparison with other methods

Current mouse models of metastasis are too expensive and time consuming to use for rapid and high-throughput screening [19,20]. Also in vitro model of metastatic dissemination such as a Boyden chamber assay can test a limited number of chemicals in one assay and needs huge times and efforts in analyzing the results[21]. Therefore, the discovery of anti-metastatic drugs is based essentially on accumulated knowledge of the molecular mechanisms of metastasis: identifying therapeutic targets for inhibiting metastasis, evaluating the effect of candidate chemicals and the markers which are used to measure a suppressor effect [22-24]. In contrast, our screen only needs

98 zebrafish embryos and enables 100 chemicals to be tested in five hours through just observing
99 epiboly progression of a test chemical-treated embryos. Furthermore, out of the 78 chemicals
100 which interrupt epiboly progression of zebrafish embryos, 20 of the chemicals were validated to
101 suppress cell motility and invasion of highly metastatic human cancer cells without affecting cell
102 viability in a Boyden chamber assay. Disadvantages of this screen is that 75% of the chemicals
103 which interrupt epiboly progression of zebrafish embryos, fail to suppress cell motility and
104 invasion of highly metastatic human cancer cells in a Boyden chamber assay [17].
105
106 Experimental design
107 This screen measures suppressor effect of each of chemicals based on epiboly progression of
108 zebrafish embryos. Niclosamid or DMSO is used as positive or negative control, respectively.
109 Epiboly progression of each of chemical treated embryos is compared with that of DMSO-treated
110 embryos. Firstly, embryos at two cell stage are corrected and approximately twenty embryos are
111 arranged into each well of 24-well plate. Each of chemicals are added when the embryos develop
112 to sphere stage. Suppressor effects of each of chemicals on the epiboly progression are measured
113 under stereoscopic microscope when DMSO-treated embryos develop to 90% epiboly stage [17].
114
115 Limitations
116 There is a limitation in delivering chemicals to zebrafish embryos. Zebrafish embryos are
117 surrounded by the acellular chorion, which is known to be about 1.5–2.5 μm thick and to consist
118 of three layers pierced by pore canals. The pore allows passage of water, ions, and chemicals. A
119 study reported molecules which are larger than 3-4KDa fail to pass through the chorion.
120 Therefore, this screen can not measure suppressor effect of the molecules which are larger than 3-
121 4KDa [25].
122
123 **Materials**

124 REAGENTS

125 - Wild-type AB zebrafish strain
126 - E3 medium (5.0 mM NaCl, 0.17 mM KCl, 0.33 mM $MgSO_4$)
127 - FDA, EMA, and other agencies-approved chemical libraries were purchased from
128 Prestwick Chemical (Illkirch, France).
129 - Niclosamid
130 - DMSO

131

132 EQUIPMENT

133 - 24-well flat bottom plastic plates (Corning)
134 - Stereomicroscope (MZ75, Leica)
135 - Incubator (Thermo)

136

137 **Procedure**

138 Zebrafish mating setup (Day 0) _Timing 10 mins

139 1. On the night before collecting embryos, arrange male and female zebrafish in pairs
140 separated by divider
141 CRITICAL STEP
142 Young adult zebrafish should be used for the crossing. Quality of zebrafish embryos
143 affect screening efficiency.

144 Embryo collection, and distribution (Day 1) _Timing 10-30 min

145 **2.** Remove the divider to allow the fish to spawn.
146 **3.** To obtain same development stage of zebrafish embryos, zebrafish were crossed for 10
147 mins. If more than twenty chemicals were tested, the crossing were conducted three times
148 at three different time points (Group A_8:30, Group B_9:00 and Group C_9:30AM).

149 4. After 10mins, set back divider to prevent zebrafish from spawning.

150 CRITICAL STEP

151 This screen measures suppressor effect of each of drugs by progression of epiboly in live
152 zebrafish embryos. Therefore, epiboly proceeds during measuring the effect under
153 stereoscopic microscope. If more than 20 chemicals were tested, screening should be
154 divided into more than two sessions and each of the sessions start at different time point.
155 For example, if screen test 60 chemicals, zebrafish should be crossed at three different
156 time points over 30 mins apart. To do that, 30 mins for measuring the effects would be
157 ensured.

158 5. Collect the embryos and remove dead embryos
159 6. Incubate the embryos at 27 ˚C for twenty mins and then collect embryos at two cell stage
160 under stereoscopic microscope.
161 7. Array approximately twenty embryos into each well of 24 well plate
162 8. Remove E3 medium from each well including the embryos by pipet
163 9. Add 900 µl of E3 medium water to the well.

164 Develop embryos to sphere stage_Timing 4 hours

165 10. Incubate the embryos at 27 ˚C until the embryos develop to sphere stage

166 Addition of chemicals_Timing 30 mins

167 11. Before 30 mins from adding chemicals to embryos, prepare E3 medium containing
168 chemicals. Prepare 100 µl of 10-fold concentration of chemicals-containing E3 medium
169 containing desired final concentration
170 12. Add 100 µl of the solution into each well when the embryos develop to sphere stage.
171 13. First 22 chemicals, Niclosamid as positive control, and DMSO as negative control are
172 added into group A when embryos from group A develop to sphere stage.

14. Second 22 chemicals, Niclosamid, and DMSO were added into group B when embryos from group B develop to sphere stage.
15. Last 22 chemicals, Niclosamid, and DMSO were added into group C when embryos from group C develop to sphere stage

Develop DMSO-treated embryos to 90% epiboly stage_Timing 5 hours

16. After the addition of chemicals, the embryos were incubated at 27 ˚C for approximately five hours

Measuring the inhibition effects of each of chemicals_Timing 30 mins

17. Comparing epiboly progression of each of chemicals-treated embryos from group A with that of DMSO-treated embryos from group A under stereoscopic microscope when DMSO-treated embryos from group A develop to 90% epiboly stage.
18. After approximately 30 mis from observing embryos from group A, measuring the inhibition effects of each of chemicals on epiboly progression of embryos from group B and when DMSO-treated embryos from group B develop to 90% epiboly stage.
19. After approximately 30 mis from observing embryos from group B, measuring the inhibition effects of each of chemicals on epiboly progression of embryos from group C and when DMSO-treated embryos from group C develop to 90% epiboly stage.

Timing

Step 1, Zebrafish mating setup: overnight

Step 2-4, Crossing zebrafish: 10 mins

Step 5+6, Collect two cell stage embryos: 20 mins

Step 7-9, Array 20 embryos into each well of 24-well plate: 30 mins

Step 10, Develop the embryos to sphere stage: 4 hours

198 Step 11-15, Prepare chemical drugs and add the solution into each well of 24-well plate: 30 mins

199 Step 16, Develop the embryos to 90% epiboly stage: 5 hours

200 Step 17-19, measuring epiboly progression: 30 mins

201

202 **Troubleshooting**

203 Quality of zebrafish embryos affect screening efficiency. A study which investigates
204 development of 12,919 fertilized embryos from zebrafish AB line reveals that by three hours post
205 fertilization, 290 (2.3%) or 2,055 (16.3%) of the fertilized eggs die or show morphological
206 abnormalities, respectively. Low quality of zebrafish embryos would generate false 'hit'
207 chemicals since our screen measures suppressor effect of a test chemical through just observing
208 epiboly progression of the chemical-treated embryos. If the number of zebrafish embryos
209 showing morphological abnormalities correlate with final concentration of a test chemical, the
210 abnormalities may result from an effect of the test chemical on the embryos.

211

212 **Anticipated results**

213 Suppressor effects of tested chemicals on epiboly progression of zebrafish embryos are
214 significantly affected by final concentration of the chemicals. Previous study showed 0.9%
215 (12/1280) of the drugs induced severe or complete arrest of embryonic cell movement when
216 embryos were treated with 10 μM. 5.2% (66/1280) of the drugs induced either delayed epiboly or
217 interrupted epiboly of the embryos. 93.3% (1194/1280) of drugs have no effect on epiboly
218 progression of the embryos. 0.6% (8/1280) of drugs induced toxic lethality. Out of the 78
219 epiboly-interrupting drugs, 25% of the chemicals succeed to suppress cell motility and invasion
220 of highly metastatic human cancer cells in a Boyden chamber assay. In contrast, epiboly
221 progression was affected more severely when embryos were treated with 50 μM. However,
222 almost of the chemicals which interrupt epiboly progression of zebrafish embryos when embryos

223 were treated with 50 μM, failed to suppress cell motility and invasion of highly metastatic human
224 cancer cells in a Boyden chamber assay [17].
225
226 **Author contributions statements**
227 J.N. created a concept of this screen, designed research, conducted experiments, analyzed data,
228 wrote and edited original draft, supervised this project; H.M. and Z.G. administered this project,
229 acquired funding.
230
231 **ORCID for corresponding authors**
232 Joj Nakayama: ORCID: 0000-0003-1077-140X
233
234 **Acknowledgments**
235 We thank Dr. Herrick (Albany Medical College) for providing pCMV-h5TH2C-VSV with us.
236 This study was funded by grants from National Medical Research Council of Singapore (R-
237 154000547511) and Ministry of Education of Singapore (R-154000A23112) to ZG. Experiments
238 using mice were supported in part by research funds from the Yamagata prefectural government
239 and the City of Tsuruoka.
240
241 **Competing interests**
242 J.N., Z.G., and H.M. declare no conflict of interest.
243

244 **Fig. 1**

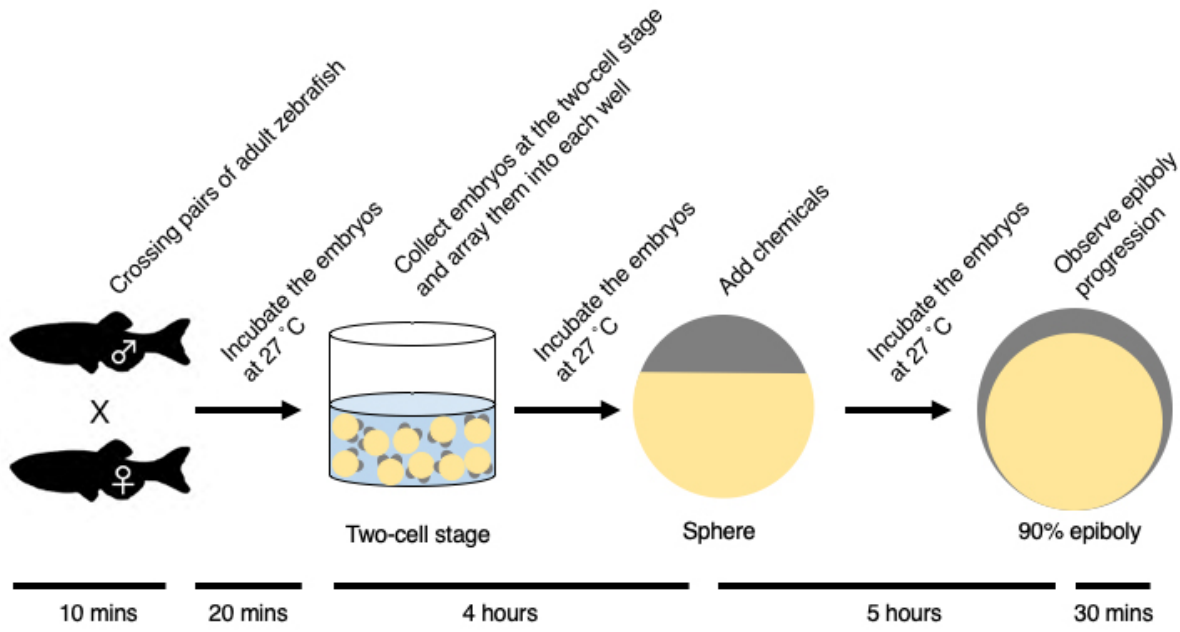

245

246 **Fig. 1_Graphic schematic of a phenotype-based chemical screen using zebrafish embryos**

247 Pairs of adult zebrafish are crossed and their embryos at two-cell stage are collected and arrayed

248 into individual wells of 24-well plate. Chemicals are added into each well when the embryos

249 develop to sphere stage. Epiboly progression of each of chemicals-treated embryos are compared

250 with that of DMSO-treated embryos under a stereoscopic microscope when DMSO-treated

251 embryos develop to 90% epiboly stage.

252

253 **Fig. 2**

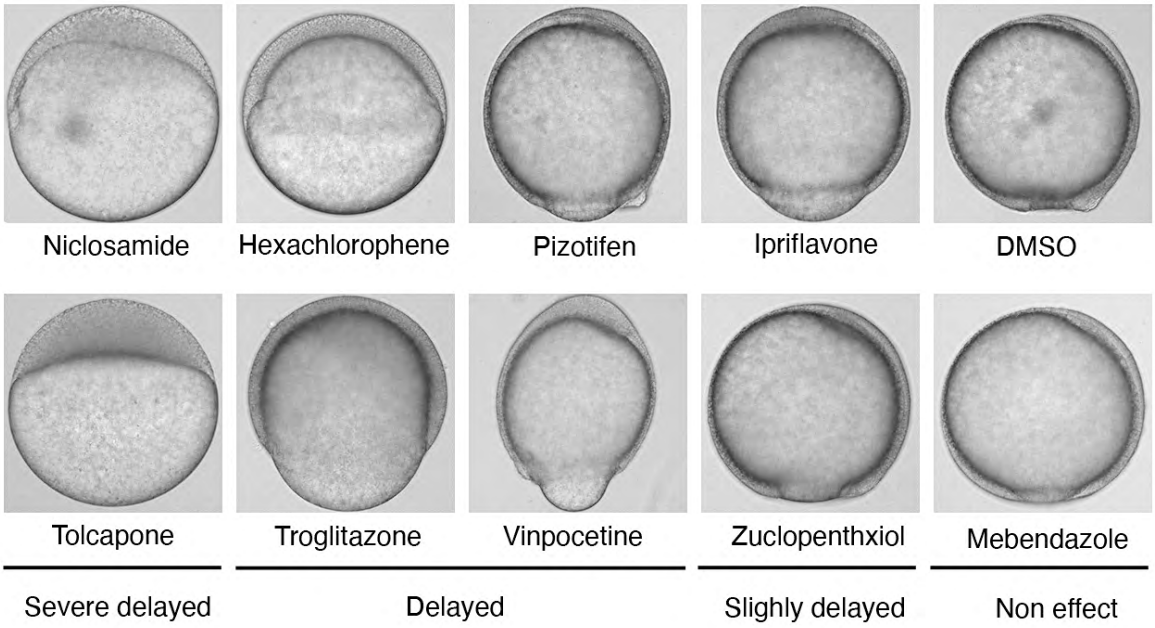

254

255 **Fig. 2_Representative samples of the embryos that were treated with indicated chemicals.**

256 Indicated chemicals were added when the embryos develop to the sphere stage. Embryos were

257 treated with 10 μM. Niclosamide-treated embryos serve as positive control and DMSO-treated

258 embryos serve as negative control. Epiboly progression of each of chemicals-treated embryos are

259 compared with that of DMSO-treated embryos under a stereoscopic microscope when DMSO-

260 treated embryos develop to 90% epiboly stage.

261 **Fig. 3**

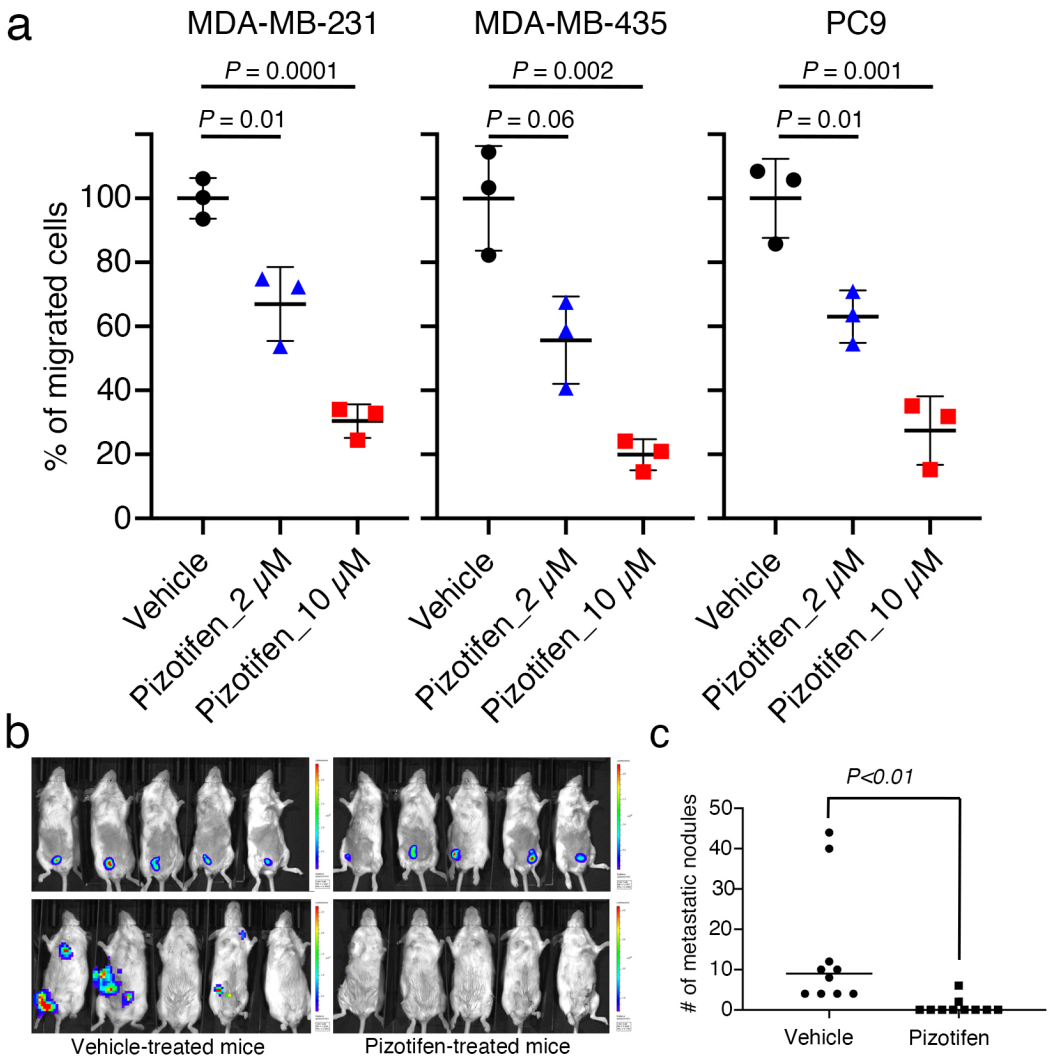

262

263 **Fig. 3_Pizotifen, one of epiboly-interrupting drugs, suppressed metastatic progression**

264 **of breast cancer cells in vitro and vivo**

265 a, Effect of pizotifen on cell motility and invasion of MBA-MB-231, MDA-MB-435, and

266 PC9 cells. Either vehicle or pizotifen treated the cells were subjected to Boyden chamber

267 assays. Fetal bovine serum (1% v/v) was used as the chemoattractant in both assays. Each

268 experiment was performed at least twice. b, Representative images of primary tumors on day

269 10 post injection (top panels) and metastatic burden on day 70 post injection (bottom panels)

270 taken using an IVIS Imaging System. c, Number of metastatic nodules in the lung of either

271 vehicle- or pizotifen-treated mice.

272

273 **Fig. 4**

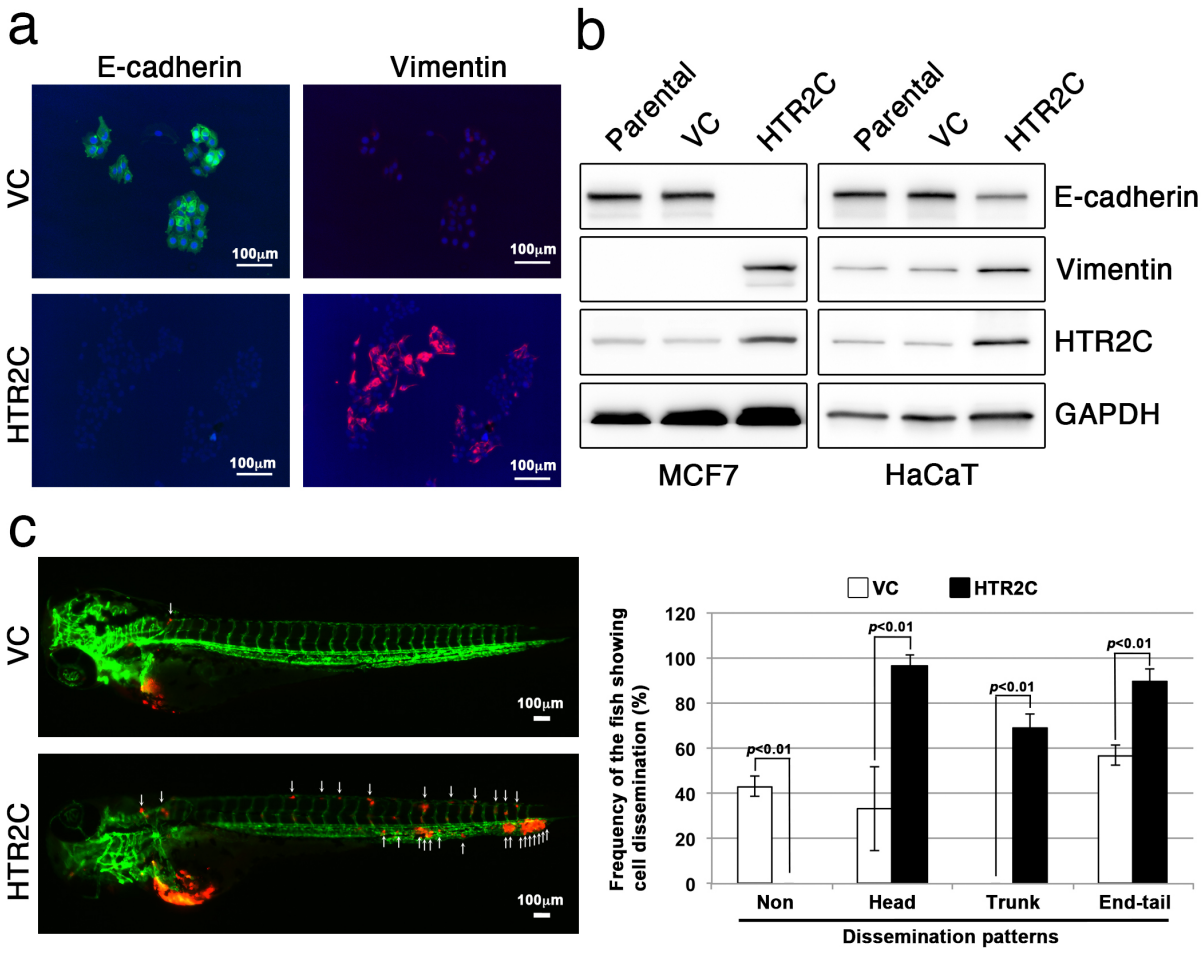

274

275 **Fig. 4_ HTR2C, a primary target of Pizotifen, induces epithelial-to-mesenchymal**

276 **transition (EMT)-mediated metastatic dissemination of human cancer cells**

277 a, Immunofluorescence staining of E-cadherin and vimentin expressions in the MCF7 cells.

278 b, Expression of E-cadherin and vimentin, and HTR2C was examined by western blotting in

279 the MCF7 and HaCaT cells; GAPDH loading control is shown (bottom). c, Representative

280 images of dissemination patterns of MCF7 cells expressing either the control vector (top left)

281 or HTR2C (lower left) in a zebrafish xenotransplantation model. White arrow heads indicate

282 disseminated MCF7 cells. The mean frequencies of the fish showing head, trunk, or end-tail

283 dissemination tabulated (right). Each value is indicated as the mean ± SEM of two

284 independent experiments. Statistical analysis was determined by Student's t test.

285 **Table 1. A list of the common fifty genes that are involved between gastrulation and**

286 **metastasis progression**

287

Genes	Gastrulation Defects	Ref	Effects in Metastasis	Ref
BMP	Convergence and extension	26	EMT	27
WNT	Convergence and extension	28	Migration and Invasion	29
FGF	Convergence and extension	30	Invision	31
EGF	Epiboly	32	Migration	33
PDGF	Convergence and extension	34	EMT	35
CXCL12	Migration of endodermal cells	36	Migration and Invasion	37
CXCR4	Migration of endodermal cells	36	Migration and Invasion	37
PIK3CA	Convergence and extension	38	Migration and Invasion	39
YES	Epiboly	40	Migration	41
FYN	Epiboly	42	Migration and Invasion	43
MAPK1	Epiboly	44	Migration	45
SHP2	Convergence and extension	46	Migration	47
SNAI1	Convergence and extension	48	EMT	49
SNAI2	Mesoderm & Neural crest formation	50	EMT	51
TWIST1	Mesoderm formation	52	EMT	53
TBXT	Convergence and extension	28	EMT	54
ZEB1	Epiboly	55	EMT	56
GSC	Mesodermal patterning	57	EMT	58
FOXC2	Unclear, defects in gastrulation	59	EMT	60
STAT3	Convergence and extension	61	Migration	62
POU5F1	Epiboly	63	EMT	64
EZH2	Unclear, defects in gastrulation	65	Invasion	66
EHMT2	Defects in Neurogenesis	67	Migration and Invasion	68
BMI1	Defects in skelton formation	69	EMT	70
RHOA	Convergence and extension	71	Migration and Invasion	72
CDC42	Convergence and extension	73	Migration and Invasion	74
RAC1	Convergence and extension	75	Migration and Invasion	76
ROCK2	Convergence and extension	77	Migration and Invasion	78
PAR1	Convergence and extension	79	Migration	80
PRKCI	Convergence and extension	79	EMT	81
CAP1	Convergence and extension	82	Migration	83
EZR	Epiboly	84	Migration	85
EPCAM	Epiboly	86	Migration and Invasion	87
ITGB1 / ITA5	Mesodermal Migration	88	Migration and Invasion	89
FN1	Convergence and extension	90	Invasion	91
HAS2	Dorsal migration of lateral cells	92	Invasion	93
MMP14	Convergence and extension	94	Invasion	95
COX1	Epiboly	96	Invasion	97
PTGES	Convergence and extension	98	Invasion	99
SLC39A6	Aterior migration	100	EMT	101
GNA12 / 13	Convergence and extension	67	Migration and Invasion	102
OGT	Epiboly	103	Migration and Invasion	104
CCN1	Cell Movement	105	Migration and Invasion	106
TRPM7	Convergence and extension	107	Migration	108
MAPKAPK2	Epiboly	109	Migration	110
B4GALT1	Convergence and extension	111	Invasion	112
IER2	Convergence and extension	113	Migration	114
TIP1	Convergence and extension	115	Migration and Invasion	116
PAK5	Convergence and extension	117	Migration	118
MARCKS	Convergence and extension	119	Migration and Invasion	120

288
289

290 References

291 1 Zon, L. I. & Peterson, R. T. In vivo drug discovery in the zebrafish *Nat Rev Drug*
292 *Discov* **4**, 35-44 (2005).
293 2 Nakayama., J., Lu., J.-W., Makinoshima., H. & Gong., Z. A Novel Zebrafish Model of
294 Metastasis Identifies the HSD11β1 Inhibitor Adrenosterone as a Suppressor of
295 Epithelial-Mesenchymal Transition and Metastatic Dissemination. *Mol Cancer Res*
296 **18**, 477-487. (2020).
297 3 Nakayama, J. & Makinoshima, H. Zebrafish-Based Screening Models for the
298 Identification of Anti-Metastatic Drugs. *Molecules* **25**, 2407 (2020).
299 4 Nakayama, J. & Gong, Z. Transgenic zebrafish for modeling hepatocellular carcinoma.
300 *MedComm* **1**, 146-156. (2020).
301 5 Nguyen., D. X., Bos., P. D. & Massagué., J. Metastasis: from dissemination to organ-
302 specific colonization. *Nat Rev Cancer* **9**, 274-284 (2009).
303 6 Welch, D. R. & Hurst, D. R. Defining the Hallmarks of Metastasis *Cancer research* **79**,
304 3011-3027. (2019).
305 7 Chaffer, C. L. & Weinberg, R. A. A perspective on cancer cell metastasis *Science* **331**,
306 1559-1564 (2011).
307 8 Lu, W. & Kang, Y. Epithelial-Mesenchymal Plasticit in Cancer Progression and
308 Metastasis. *Developmental Cell* **49**, 361-374 (2019).
309 9 Tsai, J. H. & Yang, J. Epithelial–mesenchymal plasticity in carcinoma metastasis.
310 *Genes Dev* **27**, 2192-2206 (2013).
311 10 Solnica-Krezel, L. Conserved patterns of cell movements during vertebrate
312 gastrulation *Curr Biol* **15**, R213-228. , doi:10.1016/j.cub.2005.03.016. (2005).
313 11 Yang., J., Parker, A. & Geert, B. Guidelines and definitions for research on epithelial-
314 mesenchymal transition. *Nat Rev Mol Cell Biol* **21**, 341-352 (2020).
315 12 Nieto, M. A., Huang, R. Y.-J., Jackson, R. A. & Thiery, J. P. EMT: 2016 *Cell* **166**, 21-45
316 (2016).
317 13 Thiery, J. P., Acloque, H., Huang, R. Y. J. & Nieto, M. A. Epithelial-mesenchymal
318 transitions in development and disease *Cell* **139**, 871-890 (2009).
319 14 Yang, J. & Weinberg, R. A. Epithelial-mesenchymal transition: at the crossroads of
320 development and tumor metastasis *Dev Cell* **14**, 818-829 (2008).
321 15 Dongre, A. & Weinberg, R. A. **New insights into the mechanisms of epithelial-**
322 **mesenchymal transition and implications for cancer**. *Nat Rev Mol Cell Biol* **20**, 69-84
323 (2019).
324 16 Nakayama, J. *et al.* HSD11β1 promotes EMT-mediated breast cancer metastasis.
325 *bioRxiv* **doi: https://doi.org/10.1101/2021.09.27.461934** (2021).
326 17 Nakayama, J. *et al.* A zebrafish embryo screen utilizing gastrulation identifies the
327 HTR2C inhibitor pizotifen as a suppressor of EMT-mediated metastasis. *Elife* ***10***,
328 e70151 (2021).
329 18 Nakayama, J., Konno, Y., Maruyama, A., Tomita, M. & Makinoshima, H. Cinnamon
330 bark extract suppresses metastatic dissemination of cancer cells through inhibition
331 of glycolytic metabolism *J Nat Med* (2022).
332 19 Gómez-Cuadrado, L., Tracey, N., Ma, R., Qian, B. & Brunton, V. G. Mouse models of
333 metastasis: progress and prospects *Dis Model Mech* **10**, 1061-1074. (2017).
334 20 Hoffman, R. M. Orthotopic metastatic (MetaMouse) models for discovery and
335 development of novel chemotherapy *Methods Mol Med* **111**, 297-322 (2005).

336 21 Chen, H.-C. Boyden chamber assay *Methods Mol Biol* **294**, 15-22 (2005).
337 22 Sack, U., Walther, W. & Scudiero, D. Novel effect of antihelminthic Niclosamide on
338 S100A4-mediated metastatic progression in colon cancer. *J Natl Cancer Inst* **103**,
339 1018-1036 (2011).
340 23 Itoh, K. *et al.* An essential part for Rho-associated kinase in the transcellular invasion
341 of tumor cells *Nat Med*
342
343 *. 1999 Feb;5(2):* **2**, 221-225 (1999).
344 24 Marshall, J.-C. A. *et al.* Effect of inhibition of the lysophosphatidic acid receptor 1 on
345 metastasis and metastatic dormancy in breast cancer *J Natl Cancer Inst* **104**, 1306-
346 1319 (2012).
347 25 Pelka, K. E., Henn, K., Keck, A., Sapel, B. & Braunbeck, T. Size does matter –
348 Determination of the critical molecular size for the uptake of chemicals across the
349 chorion of zebrafish (Danio rerio) embryos. *Aquatic Toxicology* **185**, 1-10 (2017).
350 26 Kondo, M. Bone morphogenetic proteins in the early development of zebrafish. *FEBS*
351 *J* **274**, 2960-2967, doi:10.1111/j.1742-4658.2007.05838.x (2007).
352 27 Katsuno, Y. *et al.* Bone morphogenetic protein signaling enhances invasion and bone
353 metastasis of breast cancer cells through Smad pathway. *Oncogene* **27**, 6322-6333,
354 doi:10.1038/onc.2008.232 (2008).
355 28 Tada, M. & Smith, J. C. Xwnt11 is a target of Xenopus Brachyury: regulation of
356 gastrulation movements via Dishevelled, but not through the canonical Wnt
357 pathway. *Development* **127**, 2227-2238 (2000).
358 29 Vincan, E. & Barker, N. The upstream components of the Wnt signalling pathway in
359 the dynamic EMT and MET associated with colorectal cancer progression. *Clin Exp*
360 *Metastasis* **25**, 657-663, doi:10.1007/s10585-008-9156-4 (2008).
361 30 Yang, X., Dormann, D., Munsterberg, A. E. & Weijer, C. J. Cell movement patterns
362 during gastrulation in the chick are controlled by positive and negative chemotaxis
363 mediated by FGF4 and FGF8. *Dev Cell* **3**, 425-437 (2002).
364 31 Nomura, S. *et al.* FGF10/FGFR2 signal induces cell migration and invasion in
365 pancreatic cancer. *Br J Cancer* **99**, 305-313, doi:10.1038/sj.bjc.6604473 (2008).
366 32 Song, S. *et al.* Pou5f1-dependent EGF expression controls E-cadherin endocytosis,
367 cell adhesion, and zebrafish epiboly movements. *Dev Cell* **24**, 486-501,
368 doi:10.1016/j.devcel.2013.01.016 (2013).
369 33 Lu, Z., Jiang, G., Blume-Jensen, P. & Hunter, T. Epidermal growth factor-induced
370 tumor cell invasion and metastasis initiated by dephosphorylation and
371 downregulation of focal adhesion kinase. *Mol Cell Biol* **21**, 4016-4031,
372 doi:10.1128/MCB.21.12.4016-4031.2001 (2001).
373 34 Damm, E. W. & Winklbauer, R. PDGF-A controls mesoderm cell orientation and radial
374 intercalation during Xenopus gastrulation. *Development* **138**, 565-575,
375 doi:10.1242/dev.056903 (2011).
376 35 Jechlinger, M. *et al.* Autocrine PDGFR signaling promotes mammary cancer
377 metastasis. *J Clin Invest* **116**, 1561-1570, doi:10.1172/JCI24652 (2006).
378 36 Mizoguchi, T., Verkade, H., Heath, J. K., Kuroiwa, A. & Kikuchi, Y. Sdf1/Cxcr4 signaling
379 controls the dorsal migration of endodermal cells during zebrafish gastrulation.
380 *Development* **135**, 2521-2529, doi:10.1242/dev.020107 (2008).

381 37 Shen, H. B., Gu, Z. Q., Jian, K. & Qi, J. CXCR4-mediated Stat3 activation is essential for
382 CXCL12-induced cell invasion in bladder cancer. *Tumour Biol* **34**, 1839-1845,
383 doi:10.1007/s13277-013-0725-z (2013).
384 38 Montero, J.-A., Kilian, B., Chan, J., Bayliss, P. E. & Heisenberg, C.-P. Phosphoinositide
385 3-Kinase Is Required for Process Outgrowth and Cell Polarization of Gastrulating
386 Mesendodermal Cells. *Current Biology* **13**, 1279-1289, doi:10.1016/s0960-
387 9822(03)00505-0 (2003).
388 39 Wander, S. A. *et al.* PI3K/mTOR inhibition can impair tumor invasion and metastasis
389 in vivo despite a lack of antiproliferative action in vitro: implications for targeted
390 therapy. *Breast Cancer Res Treat* **138**, 369-381, doi:10.1007/s10549-012-2389-6
391 (2013).
392 40 Tsai, W. B., Zhang, X., Sharma, D., Wu, W. & Kinsey, W. H. Role of Yes kinase during
393 early zebrafish development. *Dev Biol* **277**, 129-141,
394 doi:10.1016/j.ydbio.2004.08.052 (2005).
395 41 Barraclough, J., Hodgkinson, C., Hogg, A., Dive, C. & Welman, A. Increases in c-Yes
396 Expression Level and Activity Promote Motility But Not Proliferation of Human
397 Colorectal Carcinoma Cells. *Neoplasia* **9**, 745-IN732, doi:10.1593/neo.07442 (2007).
398 42 Sharma, D., Holets, L., Zhang, X. & Kinsey, W. H. Role of Fyn kinase in signaling
399 associated with epiboly during zebrafish development. *Dev Biol* **285**, 462-476,
400 doi:10.1016/j.ydbio.2005.07.018 (2005).
401 43 Yadav, V. & Denning, M. F. Fyn is induced by Ras/PI3K/Akt signaling and is required
402 for enhanced invasion/migration. *Mol Carcinog* **50**, 346-352, doi:10.1002/mc.20716
403 (2011).
404 44 Krens, S. F. *et al.* Distinct functions for ERK1 and ERK2 in cell migration processes
405 during zebrafish gastrulation. *Dev Biol* **319**, 370-383,
406 doi:10.1016/j.ydbio.2008.04.032 (2008).
407 45 Radtke, S., Milanovic, M. & Rossé, C. ERK2 but not ERK1 mediates HGF-induced
408 motility in non-small cell lung carcinoma cell lines. *J Cell Sci.* **126**, 2381-2391 (2013).
409 46 Jopling, C., van Geemen, D. & den Hertog, J. Shp2 knockdown and Noonan/LEOPARD
410 mutant Shp2-induced gastrulation defects. *PLoS Genet* **3**, e225,
411 doi:10.1371/journal.pgen.0030225 (2007).
412 47 Wang, F. M. *et al.* SHP-2 promoting migration and metastasis of MCF-7 with loss of
413 E-cadherin, dephosphorylation of FAK and secretion of MMP-9 induced by IL-1beta
414 in vivo and in vitro. *Breast Cancer Res Treat* **89**, 5-14, doi:10.1007/s10549-004-1002-
415 z (2005).
416 48 Ip, Y. T. & Gridley, T. Cell movements during gastrulation: snail dependent and
417 independent pathways. *Curr Opin Genet Dev* **12**, 423-429 (2002).
418 49 Batlle, E., Sancho, E., Francí, C., Domínguez, D. & Monfar, M. The transcription factor
419 snail is a repressor of E-cadherin gene expression in epithelial tumour cells. *Nat Cell
420 Biol* **2**, 84-89 (2000).
421 50 Shi, J., Severson, C., Yang, J., Wedlich, D. & Klymkowsky, M. W. Snail2 controls
422 mesodermal BMP/Wnt induction of neural crest. *Development* **138**, 3135-3145,
423 doi:10.1242/dev.064394 (2011).
424 51 Medici, D., Hay, E. D. & B.R., O. Snail and Slug Promote Epithelial-Mesenchymal
425 Transition through □-Catenin–T-Cell Factor-4-dependent Expression of Transforming
426 Growth Factor-□3. *Molecular Biology of the Cell* **19**, 4875–4887,
427 doi:10.1091/mbc.E08 (2008).

428 52 Castanon, I. & Baylies, M. K. A Twist in fate: evolutionary comparison of Twist
429 structure and function. *Gene* **287**, 11-22 (2002).
430 53 Yang, J. *et al.* Twist, a master regulator of morphogenesis, plays an essential role in
431 tumor metastasis. *Cell* **117**, 927-939, doi:10.1016/j.cell.2004.06.006 (2004).
432 54 Fernando, R. I. *et al.* The T-box transcription factor Brachyury promotes epithelial-
433 mesenchymal transition in human tumor cells. *J Clin Invest* **120**, 533-544,
434 doi:10.1172/JCI38379 (2010).
435 55 Vannier, C., Mock, K., Brabletz, T. & Driever, W. Zeb1 regulates E-cadherin and
436 Epcam (epithelial cell adhesion molecule) expression to control cell behavior in early
437 zebrafish development. *J Biol Chem* **288**, 18643-18659,
438 doi:10.1074/jbc.M113.467787 (2013).
439 56 Spaderna, S. *et al.* The transcriptional repressor ZEB1 promotes metastasis and loss
440 of cell polarity in cancer. *Cancer Res* **68**, 537-544, doi:10.1158/0008-5472.CAN-07-
441 5682 (2008).
442 57 Sander, V., Reversade, B. & De Robertis, E. M. The opposing homeobox genes
443 Goosecoid and Vent1/2 self-regulate Xenopus patterning. *EMBO J* **26**, 2955-2965,
444 doi:10.1038/sj.emboj.7601705 (2007).
445 58 Hartwell, K. A. *et al.* The Spemann organizer gene, Goosecoid, promotes tumor
446 metastasis. *Proc Natl Acad Sci U S A* **103**, 18969-18974,
447 doi:10.1073/pnas.0608636103 (2006).
448 59 Wilm, B., James, R. G., Schultheiss, T. M. & Hogan, B. L. The forkhead genes, Foxc1
449 and Foxc2, regulate paraxial versus intermediate mesoderm cell fate. *Dev Biol* **271**,
450 176-189, doi:10.1016/j.ydbio.2004.03.034 (2004).
451 60 Mani, S. A. *et al.* Mesenchyme Forkhead 1 (FOXC2) plays a key role in metastasis and
452 is associated with aggressive basal-like breast cancers. *Proc Natl Acad Sci U S A* **104**,
453 10069-10074, doi:10.1073/pnas.0703900104 (2007).
454 61 Miyagi, C. *et al.* STAT3 noncell-autonomously controls planar cell polarity during
455 zebrafish convergence and extension. *J Cell Biol* **166**, 975-981,
456 doi:10.1083/jcb.200403110 (2004).
457 62 Abdulghani, J. *et al.* Stat3 promotes metastatic progression of prostate cancer. *Am J*
458 *Pathol* **172**, 1717-1728, doi:10.2353/ajpath.2008.071054 (2008).
459 63 Lachnit, M., Kur, E. & Driever, W. Alterations of the cytoskeleton in all three
460 embryonic lineages contribute to the epiboly defect of Pou5f1/Oct4 deficient MZspg
461 zebrafish embryos. *Dev Biol* **315**, 1-17, doi:10.1016/j.ydbio.2007.10.008 (2008).
462 64 Dai, X. *et al.* OCT4 regulates epithelial-mesenchymal transition and its knockdown
463 inhibits colorectal cancer cell migration and invasion. *Oncol Rep* **29**, 155-160,
464 doi:10.3892/or.2012.2086 (2013).
465 65 O'Carroll, D. *et al.* The polycomb-group gene Ezh2 is required for early mouse
466 development. *Mol Cell Biol* **21**, 4330-4336, doi:10.1128/MCB.21.13.4330-4336.2001
467 (2001).
468 66 Ren, G. *et al.* Polycomb protein EZH2 regulates tumor invasion via the transcriptional
469 repression of the metastasis suppressor RKIP in breast and prostate cancer. *Cancer*
470 *Res* **72**, 3091-3104, doi:10.1158/0008-5472.CAN-11-3546 (2012).
471 67 Lin, F. *et al.* Essential roles of G{alpha}12/13 signaling in distinct cell behaviors
472 driving zebrafish convergence and extension gastrulation movements. *J Cell Biol* **169**,
473 777-787, doi:10.1083/jcb.200501104 (2005).

474 68 Chen, M. W. *et al.* H3K9 histone methyltransferase G9a promotes lung cancer
475 invasion and metastasis by silencing the cell adhesion molecule Ep-CAM. *Cancer Res*
476 **70**, 7830-7840, doi:10.1158/0008-5472.CAN-10-0833 (2010).
477 69 van der Lugt, N. M. *et al.* Posterior transformation, neurological abnormalities, and
478 severe hematopoietic defects in mice with a targeted deletion of the bmi-1 proto-
479 oncogene. *Genes Dev* **8**, 757-769 (1994).
480 70 Guo, B. H. *et al.* Bmi-1 promotes invasion and metastasis, and its elevated expression
481 is correlated with an advanced stage of breast cancer. *Mol Cancer* **10**, 10,
482 doi:10.1186/1476-4598-10-10 (2011).
483 71 Zhu, S., Liu, L., Korzh, V., Gong, Z. & Low, B. C. RhoA acts downstream of Wnt5 and
484 Wnt11 to regulate convergence and extension movements by involving effectors
485 Rho kinase and Diaphanous: use of zebrafish as an in vivo model for GTPase
486 signaling. *Cell Signal* **18**, 359-372, doi:10.1016/j.cellsig.2005.05.019 (2006).
487 72 Yoshioka, K., Nakamori, S. & Itoh, K. Overexpression of small GTP-binding protein
488 RhoA promotes invasion of tumor cells. *Cancer Res* **59**, 2004-2010 (1999).
489 73 Choi, S. C. & Han, J. K. Xenopus Cdc42 regulates convergent extension movements
490 during gastrulation through Wnt/Ca2+ signaling pathway. *Dev Biol* **244**, 342-357,
491 doi:10.1006/dbio.2002.0602 (2002).
492 74 Reymond, N. *et al.* Cdc42 promotes transendothelial migration of cancer cells
493 through beta1 integrin. *J Cell Biol* **199**, 653-668, doi:10.1083/jcb.201205169 (2012).
494 75 Habas, R., Dawid, I. B. & He, X. Coactivation of Rac and Rho by Wnt/Frizzled signaling
495 is required for vertebrate gastrulation. . *Genes Dev* **17**, 295-309., doi:10.1101/
496 (2003).
497 76 Vega, F. M. & Ridley, A. J. Rho GTPases in cancer cell biology. *FEBS Lett* **582**, 2093-
498 2101, doi:10.1016/j.febslet.2008.04.039 (2008).
499 77 Marlow, F., Topczewski, J., Sepich, D. & Solnica-Krezel, L. Zebrafish Rho kinase 2 acts
500 downstream of Wnt11 to mediate cell polarity and effective convergence and
501 extension movements. *Curr Biol* **12**, 876-884 (2002).
502 78 Itoh, K. *et al.* An essential part for Rho-associated kinase in the transcellular invasion
503 of tumor cells. *Nat Med* **5**, 221-225, doi:10.1038/5587 (1999).
504 79 Kusakabe, M. & Nishida, E. The polarity-inducing kinase Par-1 controls Xenopus
505 gastrulation in cooperation with 14-3-3 and aPKC. *EMBO J* **23**, 4190-4201,
506 doi:10.1038/sj.emboj.7600381 (2004).
507 80 Shi, X., Gangadharan, B., Brass, L. F., Ruf, W. & Mueller, B. M. Protease-activated
508 receptors (PAR1 and PAR2) contribute to tumor cell motility and metastasis. *Mol*
509 *Cancer Res* **2**, 395-402 (2004).
510 81 Gunaratne, A., Thai, B. L. & Di Guglielmo, G. M. Atypical protein kinase C
511 phosphorylates Par6 and facilitates transforming growth factor beta-induced
512 epithelial-to-mesenchymal transition. *Mol Cell Biol* **33**, 874-886,
513 doi:10.1128/MCB.00837-12 (2013).
514 82 Seifert, K., Ibrahim, H., Stodtmeister, T., Winklbauer, R. & Niessen, C. M. An
515 adhesion-independent, aPKC-dependent function for cadherins in morphogenetic
516 movements. *J Cell Sci* **122**, 2514-2523, doi:10.1242/jcs.042796 (2009).
517 83 Yamazaki, K. *et al.* Adenylate cyclase-associated protein 1 overexpressed in
518 pancreatic cancers is involved in cancer cell motility. *Lab Invest* **89**, 425-432,
519 doi:10.1038/labinvest.2009.5 (2009).

520 84 Link, V. *et al.* Identification of regulators of germ layer morphogenesis using
521 proteomics in zebrafish. *J Cell Sci* **119**, 2073-2083, doi:10.1242/jcs.02928 (2006).
522 85 Khanna, C. *et al.* The membrane-cytoskeleton linker ezrin is necessary for
523 osteosarcoma metastasis. *Nat Med* **10**, 182-186, doi:10.1038/nm982 (2004).
524 86 Slanchev, K. *et al.* The epithelial cell adhesion molecule EpCAM is required for
525 epithelial morphogenesis and integrity during zebrafish epiboly and skin
526 development. *PLoS Genet* **5**, e1000563, doi:10.1371/journal.pgen.1000563 (2009).
527 87 Ni, J. *et al.* Role of the EpCAM (CD326) in prostate cancer metastasis and
528 progression. *Cancer Metastasis Rev* **31**, 779-791, doi:10.1007/s10555-012-9389-1
529 (2012).
530 88 Skalski, M., Alfandari, D. & Darribere, T. A key function for alphav containing
531 integrins in mesodermal cell migration during Pleurodeles waltl gastrulation. *Dev Biol*
532 **195**, 158-173, doi:10.1006/dbio.1997.8838 (1998).
533 89 Felding-Habermann, B. Integrin adhesion receptors in tumor metastasis. *Clin Exp*
534 *Metastasis* **20**, 203-213 (2003).
535 90 Marsden, M. & DeSimone, D. W. Integrin-ECM Interactions Regulate Cadherin-
536 Dependent Cell Adhesion and Are Required for Convergent Extension in Xenopus.
537 *Current Biology* **13**, 1182-1191, doi:10.1016/s0960-9822(03)00433-0 (2003).
538 91 Malik, G. *et al.* Plasma fibronectin promotes lung metastasis by contributions to
539 fibrin clots and tumor cell invasion. *Cancer Res* **70**, 4327-4334, doi:10.1158/0008-
540 5472.CAN-09-3312 (2010).
541 92 Bakkers, J. *et al.* Has2 is required upstream of Rac1 to govern dorsal migration of
542 lateral cells during zebrafish gastrulation. *Development* **131**, 525-537,
543 doi:10.1242/dev.00954 (2004).
544 93 Kim, H. R. *et al.* Hyaluronan facilitates invasion of colon carcinoma cells in vitro via
545 interaction with CD44. *Cancer Res* **64**, 4569-4576, doi:10.1158/0008-5472.CAN-04-
546 0202 (2004).
547 94 Coyle, R. C., Latimer, A. & Jessen, J. R. Membrane-type 1 matrix metalloproteinase
548 regulates cell migration during zebrafish gastrulation: evidence for an interaction
549 with non-canonical Wnt signaling. *Exp Cell Res* **314**, 2150-2162,
550 doi:10.1016/j.yexcr.2008.03.010 (2008).
551 95 Perentes, J. Y. *et al.* Cancer cell-associated MT1-MMP promotes blood vessel
552 invasion and distant metastasis in triple-negative mammary tumors. *Cancer Res* **71**,
553 4527-4538, doi:10.1158/0008-5472.CAN-10-4376 (2011).
554 96 Cha, Y. I. *et al.* Cyclooxygenase-1-derived PGE2 promotes cell motility via the G-
555 protein-coupled EP4 receptor during vertebrate gastrulation. *Genes Dev* **20**, 77-86,
556 doi:10.1101/gad.1374506 (2006).
557 97 Kundu, N. & Fulton, A. M. Selective cyclooxygenase (COX)-1 or COX-2 inhibitors
558 control metastatic disease in a murine model of breast cancer. *Cancer Res* **62**, 2343-
559 2346 (2002).
560 98 Speirs, C. K. *et al.* Prostaglandin Gbetagamma signaling stimulates gastrulation
561 movements by limiting cell adhesion through Snai1a stabilization. *Development* **137**,
562 1327-1337, doi:10.1242/dev.045971 (2010).
563 99 Wang, D. & Dubois, R. N. Prostaglandins and cancer. *Gut* **55**, 115-122,
564 doi:10.1136/gut.2004.047100 (2006).

565 100 Yamashita, S. *et al.* Zinc transporter LIVI controls epithelial-mesenchymal transition
566 in zebrafish gastrula organizer. *Nature* **429**, 298-302, doi:10.1038/nature02545
567 (2004).
568 101 Lue, H. W. *et al.* LIV-1 promotes prostate cancer epithelial-to-mesenchymal
569 transition and metastasis through HB-EGF shedding and EGFR-mediated ERK
570 signaling. *PLoS One* **6**, e27720, doi:10.1371/journal.pone.0027720 (2011).
571 102 Yagi, H. *et al.* A synthetic biology approach reveals a CXCR4-G13-Rho signaling axis
572 driving transendothelial migration of metastatic breast cancer cells. *Sci Signal* **4**,
573 ra60, doi:10.1126/scisignal.2002221 (2011).
574 103 Webster, D. M. *et al.* O-GlcNAc modifications regulate cell survival and epiboly
575 during zebrafish development. *BMC Dev Biol* **9**, 28, doi:10.1186/1471-213X-9-28
576 (2009).
577 104 Lynch, T. P. *et al.* Critical role of O-Linked beta-N-acetylglucosamine transferase in
578 prostate cancer invasion, angiogenesis, and metastasis. *J Biol Chem* **287**, 11070-
579 11081, doi:10.1074/jbc.M111.302547 (2012).
580 105 Latinkic, B. V. Xenopus Cyr61 regulates gastrulation movements and modulates Wnt
581 signalling. *Development* **130**, 2429-2441, doi:10.1242/dev.00449 (2003).
582 106 Lin, J. *et al.* A novel anti-Cyr61 antibody inhibits breast cancer growth and metastasis
583 in vivo. *Cancer Immunol Immunother* **61**, 677-687, doi:10.1007/s00262-011-1135-y
584 (2012).
585 107 Liu, W. *et al.* TRPM7 regulates gastrulation during vertebrate embryogenesis. *Dev*
586 *Biol* **350**, 348-357, doi:10.1016/j.ydbio.2010.11.034 (2011).
587 108 Middelbeek, J. *et al.* TRPM7 is required for breast tumor cell metastasis. *Cancer Res*
588 **72**, 4250-4261, doi:10.1158/0008-5472.CAN-11-3863 (2012).
589 109 Holloway, B. A. *et al.* A novel role for MAPKAPK2 in morphogenesis during zebrafish
590 development. *PLoS Genet* **5**, e1000413, doi:10.1371/journal.pgen.1000413 (2009).
591 110 Kumar, B. *et al.* p38 mitogen-activated protein kinase-driven MAPKAPK2 regulates
592 invasion of bladder cancer by modulation of MMP-2 and MMP-9 activity. *Cancer Res*
593 **70**, 832-841, doi:10.1158/0008-5472.CAN-09-2918 (2010).
594 111 Machingo, Q. J., Fritz, A. & Shur, B. D. A beta1,4-galactosyltransferase is required for
595 convergent extension movements in zebrafish. *Dev Biol* **297**, 471-482,
596 doi:10.1016/j.ydbio.2006.05.024 (2006).
597 112 Zhu, X. *et al.* Elevated beta1,4-galactosyltransferase I in highly metastatic human
598 lung cancer cells. Identification of E1AF as important transcription activator. *J Biol*
599 *Chem* **280**, 12503-12516, doi:10.1074/jbc.M413631200 (2005).
600 113 Hong, S. K., Tanegashima, K. & Dawid, I. B. XIer2 is required for convergent extension
601 movements during Xenopus development. *Int J Dev Biol* **55**, 917-921,
602 doi:10.1387/ijdb.113288sh (2011).
603 114 Neeb, A. *et al.* The immediate early gene Ier2 promotes tumor cell motility and
604 metastasis, and predicts poor survival of colorectal cancer patients. *Oncogene* **31**,
605 3796-3806, doi:10.1038/onc.2011.535 (2012).
606 115 Besser, J., Leito, J. T., van der Meer, D. L. & Bagowski, C. P. Tip-1 induces filopodia
607 growth and is important for gastrulation movements during zebrafish development.
608 *Dev Growth Differ* **49**, 205-214, doi:10.1111/j.1440-169X.2007.00921.x (2007).
609 116 Han, M., Wang, H., Zhang, H. T. & Han, Z. The PDZ protein TIP-1 facilitates cell
610 migration and pulmonary metastasis of human invasive breast cancer cells in

611 athymic mice. *Biochem Biophys Res Commun* **422**, 139-145,
612 doi:10.1016/j.bbrc.2012.04.123 (2012).
613 117 Faure, S. *et al.* Xenopus p21-activated kinase 5 regulates blastomeres' adhesive
614 properties during convergent extension movements. *Dev Biol* **277**, 472-492,
615 doi:10.1016/j.ydbio.2004.10.005 (2005).
616 118 Gong, W. *et al.* P21-activated kinase 5 is overexpressed during colorectal cancer
617 progression and regulates colorectal carcinoma cell adhesion and migration. *Int J*
618 *Cancer* **125**, 548-555, doi:10.1002/ijc.24428 (2009).
619 119 Iioka, H., Ueno, N. & Kinoshita, N. Essential role of MARCKS in cortical actin dynamics
620 during gastrulation movements. *J Cell Biol* **164**, 169-174, doi:10.1083/jcb.200310027
621 (2004).
622 120 Rombouts, K. *et al.* Myristoylated Alanine-Rich protein Kinase C Substrate (MARCKS)
623 expression modulates the metastatic phenotype in human and murine colon
624 carcinoma in vitro and in vivo. *Cancer Lett* **333**, 244-252,
625 doi:10.1016/j.canlet.2013.01.040 (2013).
626